Single-Walled Carbon Nanotubes (SWCNTs)-Assisted Cell-Systematic Evolution of Ligands by Exponential Enrichment (Cell-SELEX) for Improving Screening Efficiency

ARTICLE *in* ANALYTICAL CHEMISTRY · SEPTEMBER 2014

Impact Factor: 5.64 · DOI: 10.1021/ac502166b · Source: PubMed

12 AUTHORS, INCLUDING:

Yuyu Tan
Hunan University
10 PUBLICATIONS **29** CITATIONS
SEE PROFILE

Jianbo Liu
Hunan University
37 PUBLICATIONS **381** CITATIONS
SEE PROFILE

Xiaoxiao He
Hunan University
150 PUBLICATIONS **3,715** CITATIONS
SEE PROFILE

Xiaohai Yang
Hunan University
158 PUBLICATIONS **2,211** CITATIONS
SEE PROFILE

analytical chemistry

Article

pubs.acs.org/ac

Single-Walled Carbon Nanotubes (SWCNTs)-Assisted Cell-Systematic Evolution of Ligands by Exponential Enrichment (Cell-SELEX) for Improving Screening Efficiency

Yuyu Tan,† Qiuping Guo,† Qin Xie, Kemin Wang,* Baoyin Yuan, Yu Zhou, Jianbo Liu, Jin Huang, Xiaoxiao He, Xiaohai Yang, Chunmei He, and Xiayu Zhao

State Key Laboratory of Chemo/Biosensing and Chemometrics, College of Biology, College of Chemistry and Chemical Engineering, and Key Laboratory for Bio-Nanotechnology and Molecule Engineering of Hunan Province, Hunan University, Changsha 410082, China

Supporting Information

ABSTRACT: Separating the specific from the nonspecific bound single-strand DNA (ssDNA) is the most important step to improve the efficiency of selection procedure. However, most cell-SELEX protocols (where SELEX = systematic evolution of ligands by exponential enrichment) use simply washing only, which leads to incomplete separation. It is well-established that ssDNAs can be adsorbed on single-walled carbon nanotubes (SWCNTs). Based on this, herein, we developed a modified cell-SELEX approach termed "SWCNTs-assisted cell-SELEX". In our approach, SWCNTs are applied in the separation step, during which the unbound or the nonspecific ssDNAs are adsorbed onto SWCNTs, while the bound ssDNAs still remain on the cell surface, because of the stronger interaction between ssDNA and target. The cells can then be centrifuged to enrich the specifically binding aptamers. As a proof of concept, two nasopharyngeal carcinoma (NPC) cell lines—CNE2 cell and HONE cell—were used as the target cell and the negative cell, respectively. The result show that it takes only 6 cycles to enrich the aptamer pool through the SWCNTs-assisted cell-SELEX, which is much shorter than 15 cycles in the conventional cell-SELEX, thus improving the screening efficiency. Moreover, the achieved aptamers show high specificity and affinity with CNE2 cells, which are highly attractive for clinical diagnosis and biomedicine applications.

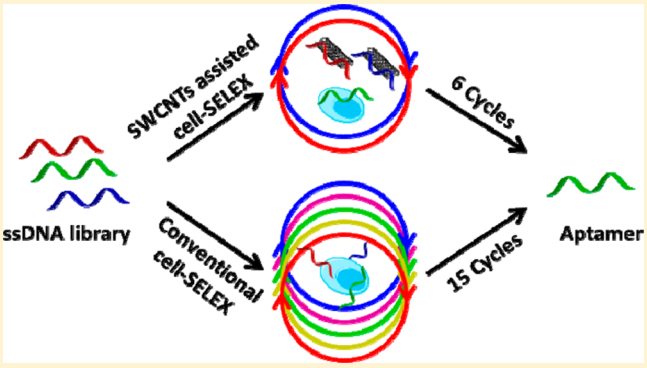

Because of its particular properties, aptamer has been widely used in the fields of environmental monitoring, bioanalytical chemistry, and biomedicine.[1,2] Aptamers are generated from Systematic Evolution of Ligands by EXponential enrichment (SELEX) process and have high affinity and specificity to targets.[3,4] In order to achieve aptamer probe for cells, the cell-SELEX strategy has been developed.[5] This process uses cells as target and select aptamers for unknown complex targets at their native conformations. In comparison to obtain the molecular probes through other methods, the cell-SELEX has several advantages, such as simple operation, direct selection, and enriching a series of aptamers simultaneously. Taking advantages of these technologies, some aptamers for cancer cells were selected in the past years, such as CCRF-CEM,[5] Ramos,[6] A549,[7] NCI-H69,[8] BNL 1MEA.7R.1,[9] HL60,[10] etc. Meanwhile, aptamers generated from cell-SELEX are effective and robust recognition elements for use in characterizing target cells on a molecular level and the applications have covered many aspects, including cancer cell detection,[11−13] cancer therapy,[14−16] and biomarker discovery.[17−19]

However, obtaining evolved aptamers via the traditional cell-SELEX method from cell-SELEX is time-consuming and laborious. Generally, ∼20 rounds of cell-SELEX are required to achieve aptamers with the highest affinity toward the target cell line.[1] Thus, it is necessary to develop a more-efficient selection procedure to achieve fast and easy aptamer screening. During the cell selection, the nonspecific adsorption of the ssDNA mainly depends on the cell surface or the container, which is tremendously amplified by the polymerase chain reaction (PCR) and lower efficiency of selection. Therefore, in the procedure of cell-SELEX, separation of the specific and nonspecific bound single-strand DNA (ssDNA) is the most important step to improve the efficiency of aptamer selection. In recent years, some excellent separation methods have been employed in aptamer selection to increase the screening efficiency. For instance, the fluorescence-activated cell sorting was applied to remove the dead cells, which have strong and nonspecific adhesion of nucleic acids.[20,21] However, these methods require specialized instruments. In addition, capillary

Received: April 1, 2014
Accepted: September 3, 2014
Published: September 3, 2014

   dx.doi.org/10.1021/ac502166b | Anal. Chem. 2014, 86, 9466−9472

electrophoresis-SELEX approach with high separation efficiency is able to significantly reduce the selection cycles to 1−3 rounds.[22−25] Unfortunately, the application of capillary electrophoresis-SELEX is limited to proteins or small molecules aptamers screening. Recently, a platform integrates magnetic bead-assisted SELEX with microfluidics technology demonstrated the capability of microsystem could isolate high-affinity aptamers after a single round of selection.[26−28] However, the selection procedure is complex and the chip is difficult to design and manipulate. Therefore, it is still in urgent demand for developing a simple and efficient cell-SELEX platform.

The carbon nanotubes, as an excellent nanomaterial, have been most extensively studied in their unique chemical, electrical, and mechanical properties.[29] Recently, it is demonstrated that ssDNAs are able to helically wrap onto SWNTs by π-stacking interactions between the nucleotide bases and SWCNT sidewalls.[30,31] Taking advantages of this unique property, some biosensors with high performance have been developed and the successful application of nanomaterials graphene oxide (GO) in aptamer selection also been achieved.[32,33] Inspired by this, we examine the possibility of employing SWCNTS in cell-SELEX to separate the unbound ssDNA and, thus, improve the selection efficiency. As proof of the concept, a modified aptamer selection approach termed "SWCNTs-assisted cell-SELEX" based on cell-SELEX and SWCNTs was developed to achieve aptamers for target cancer cell with high affinity and high specificity. In this approach, the SWCNTs are coupled into the washing step of cell-based SELEX, after incubation with target cells, the unbound or loosely bound ssDNA would be adsorbed onto the surface of the SWCNTs and be easily removed by washing, which prominently improves the separation efficiency. These novel and specific aptamers of cancer cell may provide powerful tools for tumor classification and staging, cancer cell detection, and targeting therapy.

EXPERIMENTAL SECTION

Cell Lines and Buffers. All cell lines used in this paper are human origin, including HepG2, TCA, A549, and HeLa cells, and were purchased from American Type Culture Collection. SMMC-7721, Bel-7404, and L02 were purchased from the Shanghai Institute of Cell Biology of the Chinese Academy of Science. CNE2 (target cell), HONE (subtractive control cell), EC9706, and QBC-939 were maintained at our laboratory. All of the cells were cultured in RPMI medium 1640, containing 10% FBS (heat-inactivated, GIBCO) and 100 U/mL penicillin-streptomycin (Cellgro). All cells were cultured in an incubator at 37 °C with 5% CO_2 atmosphere. The washing buffer (WB) contained 5 mM $MgCl_2$ and 4.5 g/L glucose in phosphate-buffered saline (PBS, pH 7.4). In order to reduce nonspecific binding, the binding buffer (BB) was prepared with BSA (1 mg/mL, Dingguo) and yeast tRNA (0.1 mg/mL, Sigma).

SELEX Library and Primers. All the ssDNA used in this study were designed by ourselves and synthesized by Sangon Biotech (Shanghai). The selection ssDNA library consisted of a 40 nucleotides (nt) randomized sequences and 20 nt primer sequences (5′-CGTTCGTCAGGAGTAGAGGC-40nt-CCTGCTGACTGAACCTGACG-3′). PCR (polymerase chain reaction) primer was labeled with FAM (5′-FAM-CGTTCGTCAGGAGTAGAGGC-3′) and biotin (5′-Biotin-CGTCAGGTTCAGTCAGCAGG-3′), respectively. The PCR mixtures contained 500 nM each primer, and 2X Power Taq PCR MasterMix (Bioteke). Preparation of the PCR mixtures was performed in 96-well microplates (Eppendorf, Germany), using a Laboratory Automation Workstation (Biomek 3000, America). To reduce the nonspecific amplification of PCR, the annealing temperature was optimized. Finally, the following conditions were used for PCR: 3 min at 95 °C; then, 10−20 cycles of 0.5 min at 95 °C, 0.5 min at 60 °C, and 0.5 min at 72 °C, followed by 3 min at 72 °C. After PCR, the products were incubated with the streptavidin-coated sepharose beads (GE Healthcare, America), the biotin-labeled ssDNAs were captured onto beads. The complex then was denatured with 0.2 M NaOH for 10 min; finally, the FAM-labeled ssDNAs were desalted and collected to monitor the affinity or for the next round of selection.

SWCNTs-Assisted Cell-SELEX Procedures. In the first cycle of SWCNTs-assisted cell-SELEX, a total ssDNA library of 5 nmol was used, and it was dissolved in 500 μL binding buffer and heated at 95 °C for 5 min. Finally, it was cooled immediately on ice for 10 min. The treated ssDNA library was incubated with (1−2) × 10^6 CNE2 cells on ice in a rotary shaker for 1 h as positive selection, and shaking the cells intervals for 10 min. In addition, 20% FBS and excess of random DNA were added to the incubation solution for reducing the nonspecific adsorption of cell and the container. After incubation, cells were washed with 2 mL WB three times, for 3 min each, which contained 40 μg/mL SWCNTs (Shenzhen Nanotech Port Co., Ltd.). In addition, in order to compare the efficiency of the selection, a same selection procedure without adding the SWCNTs in the washing buffer was also performed in this work. After washing, the bound DNAs were eluted by heating at 95 °C for 5 min in 500 μL ultrapure water. The eluted DNAs then were amplified by PCR and the new ssDNA library was prepared, which was described in the previous paragraph. But the difference here is that this new ssDNA library was first incubated with HONE cells (negative cells, 2-fold excess than CNE2 cells) on ice for counter selection for 1 h. Aptamers selection is generally drove by gradually enhanced condition, such as increasing the volume of WB (2−4 mL), the number of washes (1−4 times), and the time of washing (1−5 min). In addition, the incubation time with CNE2 cells was decreased from 60 min to 30 min, the incubation time with HONE cells was increased from 60 min to 90 min, and the number of cells was also increased from (1−2) × 10^6 to (5−10) × 10^6 gradually, to improve the specificity of the aptamers. After 6 or 15 rounds of selection, respectively, when the binding between target cell and ssDNA library is saturation, the ssDNA libraries were amplified by PCR with unmodified primers, then they were sent to Sangon Biotech (Shanghai) for cloning and sequencing.

Flow Cytometry Analysis. To characterize whether the selected pool is enriched, the flow cytometry was used. When the cells overspread the 90% of the culture dish, the CNE2 and HONE cells were trypsinized, then 2 × 10^5 CNE2 or HONE cells were incubated with 250 nM selected pools in 200 μL BB on ice for 30 min. Before testing, both of the CNE2 cells and the HONE cells were washed by 200 μL WB twice, 2000 rpm centrifuging at 4 °C, and the cells were suspended in 200 μL BB. Each sample was tested with the flow cytometer (FACScalibur, BD Bioscience) by counting 10 000 events. The FAM-labeled unselected ssDNA library or a random sequence was used as the negative control.

To determine the binding affinities of the aptamers, an appropriate aptamer concentration gradient was designed. Each concentration was performed for three timeshare, and the other

dx.doi.org/10.1021/ac502166b | Anal. Chem. 2014, 86, 9466−9472

procedures are similar to previous descriptions. The mean fluorescence intensity was recorded and used as the vertical axis, and the concentration of ligand was used as the horizontal axis, the K_d of the aptamer was fitted by Sigma Plot 10.0 with the one-site saturation equation

$$Y = B_{max}\left(\frac{X}{K_d + X}\right)$$

where B_{max} is the saturated binding. To investigate the specificity of aptamers for molecular recognition, positive cell lines CNE2, control cell lines HONE, SMMC-7721, QBC-939, Bel-7404, HepG2, L02, TCA, A549, Hela cells, and EC9706 were used for binding specificity assays.

Confocal Imaging of Cells Stained with Aptamers. To further confirm the specificity of achieved aptamers, the cells were imaged by a laser scanning confocal microscope (Olympus, Japan). CNE2, HONE cells were cultivated for 24 h in a culture dish, and they were washed with WB three times, then the cells were incubated with FAM-labeled aptamers or the control ssDNA library (250 nM) in BB (20% FBS) on ice for 60 min. Finally, the supernatant was removed, and the cells were washed twice WB before imaging. The FAM was excited by a 488-nm laser. The fluorescence signals were collected by a 40× objective.

Confocal Imaging of Frozen Tissue Sections Stained with Aptamers. Balb/cJ mice were inoculated with either 5×10^6 in vitro propagated CNE2 or SMMC-7721 cells into the right flank. When tumors were allowed to grow to 1−1.5 cm in diameter, then tumor tissues and normal livers tissues were cut off. After frozen fresh pieces of tumor tissue and normal liver tissue, then they were embedded in the compound; finally, 10-μm sections were produced by a cryostat, and they were fixed onto polylysine-modified glass slides. Sections were rinsed in PBS for 3 min at room temperature and used for fluorescence aptamer staining. For tissue staining, frozen sections were incubated with the control library or aptamer probes (250 nM) labeled with TAMRA in binding buffer at 4 °C for 10 min. After washing with PBS for three times, the stained sections were imaged by laser scanning confocal microscopy (Olympus, Japan). The fluorescence signals were collected using a 40× objective. The TAMRA was excited by a 488-nm laser.

RESULTS AND DISCUSSION

The Principles of SWCNTs-Assisted Cell-SELEX. The process of our SWCNTs-assisted cell-SELEX is illustrated in Figure 1. As a proof of concept, a cultured NPC cell line, CNE2, was used as the target cell for positive selection. Another NPC cell line, HONE, was used as the negative control one, to remove the aptamer bound to both type of cells; in other words, this negative selection will benefit the specificity of aptamers. In the SWCNTs-assisted cell-SELEX, an 80 nt ssDNA library has been designed, which contained two 20-nt primer regions and a 40-nt random region. The target cells then were incubated with the ssDNA library. As mentioned previously, it is well-demonstrated that ssDNAs are able to helically wrap onto SWNTs by $\pi-\pi$ stacking interactions between the nucleotide bases and SWCNT sidewalls. Here, the SWCNTs were introduced into the washing step of the cell-SELEX procedure, and added after the library was incubated with the target cell. Then, the supernatant, which contained unbound DNA or weakly bound ssDNA was discarded after centrifugation. However, the aptamers, which were still bound

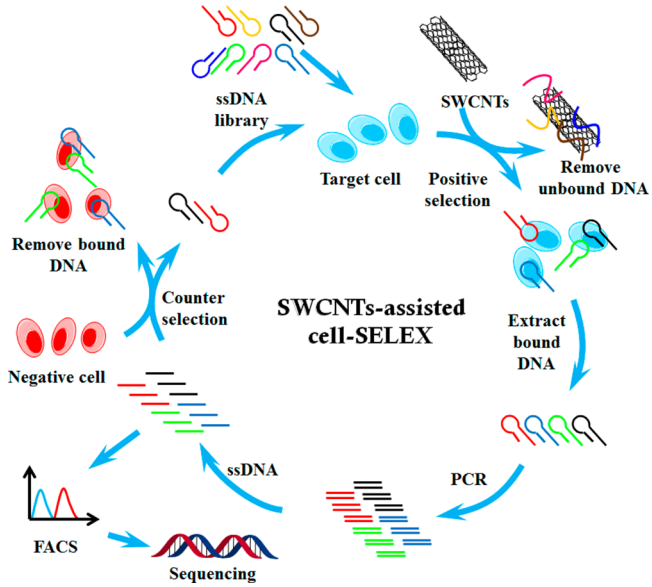

Figure 1. Schematic representation of the SWCNTs-assisted cell-SELEX.

to the cell surface, were eluted by heating. The collected ssDNAs were then amplified by PCR for the next round of selection. After several rounds of selection, the aptamer candidates were enriched, which could recognize the target cells with high specificity. Considering the impact of nanotubes on cell,[34−36] all experiments were carried on ice, and the incubation time of nanotubes and cell is shorter than 5 min; all these steps are helpful for inhibiting and reducing the affection of nanotubes on cells.

Optimization of the Ratio of ssDNA/SWCNTs. The SWCNTs used in our design were first characterized by TEM in Figure S1 in the Supporting Information, and they could be well-dispersed in water. In order to ensure complete removal of the unbound ssDNA, sufficient SWCNTs should be used in the washing step. Earlier studies have shown that a fluorophore bound to the surface of carbon nanotubes is quenched.[37,38] Herein, we confirm the minimum amount of SWCNTs by the changes in fluorescence intensity upon quenching. Therefore, different concentrations of FAM-labeled ssDNA were incubated with SWCNTs, and then the fluorescence intensity was monitored; as a result, when the ratio of ssDNA/SWCNT reached over 25.6 nmol/mg (see Figure S2 in the Supporting Information), the fluorescence had increased significantly, which indicated that the absorption of SWCNT is saturation, and this could be consisted as the minimum amount of SWCNTs, finally, 40 μg/mL of SWCNTs were used to ensure complete removal of the ssDNA.

Monitoring and Comparing the Efficiency of the SWCNTs-Assisted Cell-SELEX. The progress of the entire cell-SELEX process was monitored using flow cytometry. As expected, the fluorescence intensity on the CNE2 target cells increased as the number of selection cycles increased, and a saturated fluorescence intensity were observed after the sixth round of selection, demonstrating that the pool for recognition of CNE2 cells were enriched by the SWCNTs-assisted cell-SELEX (Figure 2A). Nevertheless, no significant changes in fluorescence intensity on the HONE control cells were observed (Figure 2B). This result demonstrated that the ssDNA pool, which specifically recognized target CNE2 cells,

dx.doi.org/10.1021/ac502166b | Anal. Chem. 2014, 86, 9466−9472

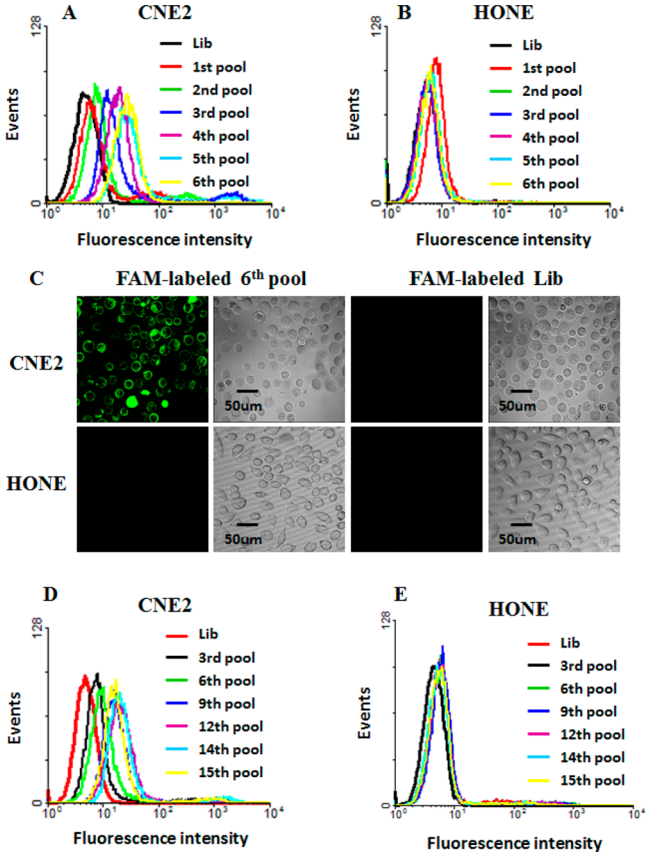

Figure 2. Flow cytometry results of selected pools with CNE2 and HONE cells. In the progress of the SWCNTs-assisted cell-SELEX, with increasing rounds of enrichment, significant increases in fluorescence intensity were detected on CNE2 cells (panel A) but not on HONE (panel B), suggesting the enrichment of CNE2 specific aptamers. (C) Confocal imaging of cells stained by the Lib or the sixth-round selected pool labeled with FAM. In the progress of the traditional cell-SELEX, by way of contrast, more cycles were needed to enrich the pool (panel D), but the pool shows good specificity for recognizing CNE2 cells (panel E).

was isolated successfully. The specific binding of the selected pools to the target cells was further confirmed by confocal imaging (Figure 2C). After incubation with FAM-labeled aptamer pool, the CNE2 cells showed very strong fluorescence on their surface, whereas the HONE cells displayed weak fluorescence. After six selection rounds by the SWCNTs-assisted cell-SELEX, highly enriched DNA pools were cloned and sequenced. Meanwhile, 15 selection rounds were needed to achieve the enriched pool with traditional cell-SELEX, compared to the SWCNTs-assisted cell-SELEX, more selection cycles are needed in the traditional cell-SELEX to enrich the pool (see Figures 2D and 2E). In addition, aptamers generated for recognizing the cell surface in other selection works (Table 1) generally require more than 12 rounds, which implies that our proposed strategy can significantly improve the efficiency of aptamer selection.

Then, the sequences were grouped and analyzed by the Clustal X and pools were aligned and phylogenetic trees were constructed (data not shown). Twenty (20) FAM-labeled sequences from the families were chosen to test whether they could bind to the target CNE2 cells by flow cytometry (data not shown). Seven sequences were chosen for further characterizing, three of them (sequences started with T) generated from SWCNTs-assisted cell-SELEX and four of them (sequences started with GP) generated from traditional cell-SELEX without SWCNTs, and all these aptamers are listed in Table 2.

Table 1. List of Some Apatamer Selection Cycles Needed in Conventional Cell-Based SELEX

cell	number of rounds	reference
CEM	~20	Shangguan et al.[5]
Ramos	~20	Tang et al.[6]
MEAR	16	Shangguan et al.[9]
A549	25	Zhao et al.[7]
SBC3	16	Kunii et al.[41]
Kato III	12	Song et al.[42]
CNE2	15	using the traditional cell-SELEX in this work
CNE2	6	using the SWCNTs-assisted cell-SELEX in this work

Recognition of the CNE2 Cells with Aptamer. After cloning and sequencing, seven aptamer candidates were chosen for further research. Moreover, flow cytometry is used to test the binding abilities of these sequences. As a result, T10, T11, and T12 show stronger fluorescence than the control probes, when bound to target cell (Figure 3A). Meanwhile, fluorescence microscopy imaging demonstrated that the aptamers specifically bound to the surface of the CNE2 cells (Figure 3B). As shown in Figure 3C, all of the aptamers displayed high binding affinities with equilibrium dissociation constants (K_d) in the nanomolar range; the K_d value for aptamers T10, T11, and T12 are 120.3 ± 1.2, 131.8 ± 2.3, and 81.4 ± 2.6, respectively. Unfortunately, the K_d value of aptamers generated by SWCNTs-assisted cell-SELEX is slightly higher than that generated by the traditional cell-SELEX; in other words, the SWCNT shows no contribution to lower their K_d values (thus, more strategies would be needed to try to improve it in the future). Incubation of aptamers with other cell lines have been tested to confirm the specificity for recognition of CNE2 cells; the three representative aptamers (T10, T11, and T12) were evaluated for the binding specificity (see Table 3). As a result, all these aptamers displayed high specificity for CNE2 cell lines. This result revealed that the aptamers may be bound to the unique cell surface proteins, and thus differentiate between NPC cells and other cancer cell or normal liver cells. Furthermore, to verify whether these aptamers are bound to the cell surface membrane proteins, the CNE2 cells were treated with trypsin or proteinase-K for 2 min and 10 min before incubation with FAM-labeled aptamers. As shown in Figure S3 in the Supporting Information, the aptamer shows similar fluorescence intensity with the unselected pool. Based on this, we can conclude that the binding sites of aptamers are membrane proteins. In addition, we incubated CNE2 cells with aptamer T11 at different temperatures to test its binding abilities. Note that aptamer T11 displayed stable binding affinities at temperatures under 4, 25, 37, and 40 °C (see Figure S4 in the Supporting Information), which further demonstrated the potential applications in clinical diagnoses.

Recognition of the CNE2 Frozen Tissue Sections with Shorter Aptamers. Longer sequences usually are not suitable for designing probes, because of the high cost involved in synthesis. Meanwhile, the needless nucleotide sequences in the aptamers may form the complex secondary structures, and result in hindering target binding. In addition, it has been reported that the shorter ssDNA owned better tissue

dx.doi.org/10.1021/ac502166b | Anal. Chem. 2014, 86, 9466−9472

Table 2. Sequences of Isolated ssDNA Aptamers and Their Binding Affinities to CNE2 Cells

aptamer	sequence	K_d (nM)
T10	TGCCACGTGTTGGTGGAGGGAAGGGTTTAGGATTTAGGGG	120.3 ± 1.2
T11	TGGACCGGAGGTTGGGGGATGGGTGTTGGATTTGGGAGGA	131.8 ± 2.3
T12	TAGCGGCACACTATGGGAGGCGGTGGGGGGTTCGGCGGTG	81.4 ± 2.6
GP1	TCTAGGAAGCAGCTTGGGGTTGGGAGGGAGGTAAGGGGG	18.2 ± 1.1
GP6	GGGATTGGCGGGTGTGTGGGATGGGATGTAGGGCAGTGAT	73.7 ± 2.9
GP25	GTCCTGGCTGCGGATTGTGTTAATGCCGTCTGTTCCTACG	31.2 ± 2.1
GP35	GGATGGGTCGGTGGGGGTGGGATGGTGGGCTGAGAGAGCG	147.5 ± 4.4

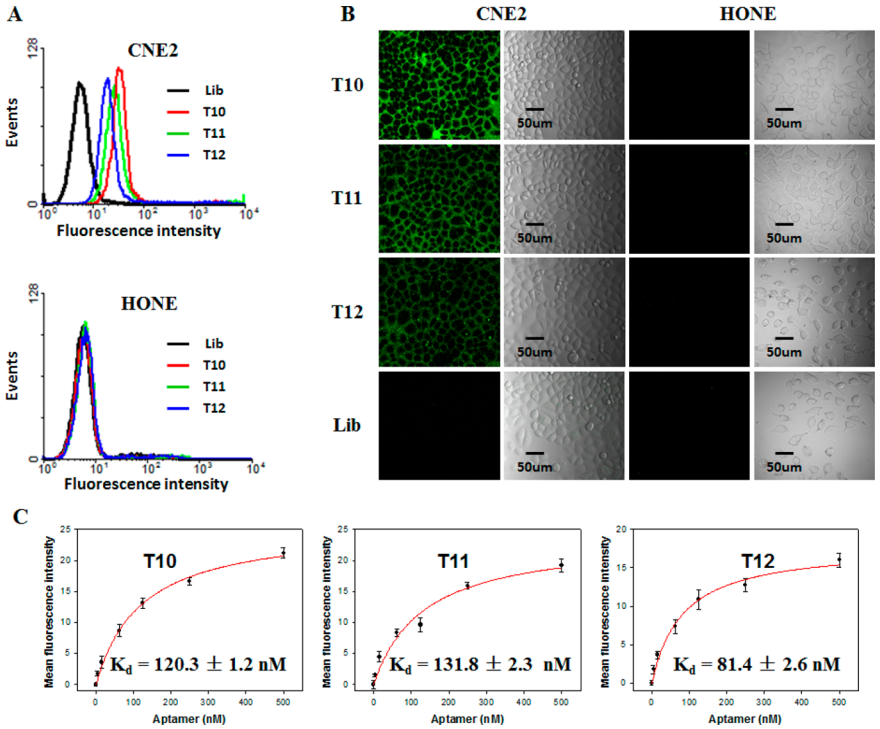

Figure 3. Characterization of selected aptamers: (A) flow cytometry assay for the binding of the FAM-labeled sequences T10, T11, and T12 with CNE2 cells (target cells) and HONE cells (negative cells) (the black curve represents the background binding of unselected DNA library, and the concentration of the aptamers in the binding buffer was 250 nM); (B) confocal imaging of cells stained by the Lib or FAM-labeled aptamer sequence T10, T11, and T12, and all the aptamers had obvious cell membrane binding property; and (C) flow cytometry to determine the binding affinity of the FAM-labeled aptamer sequence T10, T11, and T12 to CNE2 cells. The nonspecific binding was measured by using FAM-labeled unselected library DNA.

penetration ability. Therefore, shorter aptamer sequences will be more popular than the full length aptamers. In order to achieve a shorter aptamer for recognition of frozen tissue sections, we optimized the sequence of GP6, T11, and T12 according to their secondary structures analyzed by Mfold (see Figure S5A in the Supporting Information). Finally, aptamers GP47, T11a, and T12a were selected for specific recognition of CNE2 with high affinity (see Figure S5B in the Supporting Information). More importantly, these optimized aptamers showed brighter fluorescence with CNE2 tumor tissue section than the other tumor tissue section (see Figure 4). These results demonstrated that aptamers GP47, T11a, and T12a have potential applications in clinically recognized CNE2 cancer cells.

Effect of the SWCNTs on the Cell-SELEX. As previously mentioned, SWCNTs were introduced into the selection procedure, which successfully reduced the number of selection cycles from 15 to 6. In order to further evaluate the effect of SWCNTs on the selection, the binding experiment was performed by Lib or a representation of aptamer T11 to bind CNE2 cells. As shown in Figure 5A, the Lib bind to CNE2 cells with background signals without washing; after adding the appropriate SWCNTs, the signals reduced significantly, which indicated that the SWCNTs could effectively absorb the nonspecific ssDNAs. On the other hand, aptamer T11 selected by the SWCNTs-assisted cell-SELEX can bind to CNE2 cells with high affinity even in the presence of SWCNTs (Figure 5B), this result demonstrated that the existence of SWCNTs did not influence the binding between aptamer and CNE2 cells, and this further proves that the SWCNTs can be employed in the cell-SELEX as unbound ssDNA removers. In addition, we choose the SWCNT as an ssDNA remover to facilitate the SWCNTs-assisted cell-SELEX based on the following considerations. First, the ssDNA adsorption and quenching capacities of GO is weaker than that of SWCNTs under the screening conditions (see Figure S6A in the Supporting Information). Second, the desorption of ssDNAs from GO occurs more easily than SWCNT, which could directly impact the efficiency of adsorption and selection (see Figure S6B in the Supporting

dx.doi.org/10.1021/ac502166b | Anal. Chem. 2014, 86, 9466−9472

Table 3. Binding Specificity Study of Aptamers T10, T11, and T12 to Different Cancer Cell Lines, as Determined by Flow Cytometry[a]

cell	T10	T11	T12
CNE2 (target cell, nasopharyngeal carcinoma, human)	+++	++++	+++
HONE (control cell, nasopharyngeal carcinoma, human)	0	0	0
QBC-939 (cholangiocarcinoma, human)	0	0	0
L02 (hepatocyte, human)	0	0	0
SMMC-7721 (liver cancer, human)	0	0	0
HepG2 (liver cancer, human)	0	0	0
A549 (lung cancer, human)	0	0	0
Bel-7404 (liver cancer, human)	0	0	0
Hela (cervical carcinoma, human)	+	+	+
TCA (tongue cancer, human)	0	0	0
EC9706 (esophagus cancer, human)	+	+	+

[a]Note: A background fluorescence intensity of flow cytometric analysis was set so that 95% of cells stained with FAM-labeled library would have fluorescence intensity below it. The percentage of cells with fluorescence intensity above this threshold was used to evaluate the binding ability of aptamers to the cells. Legend: (0) <10%, (+) <10%−35%, (++) <35%−60%, (+++) <60−85%, and (++++) >85%.

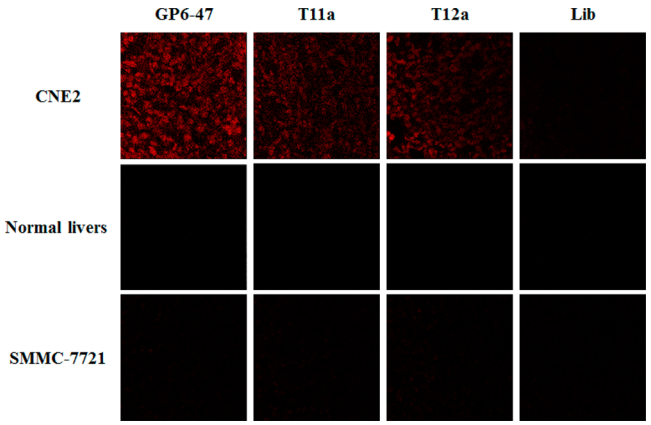

Figure 4. Laser scanning confocal microscopy was used to test the abilities of optimized aptamers for recognition of tissue slices. Fluorescence images shows that optimized aptamers GP6-47, T1s1a, and T12a were bound to CNE2 freezing slices, and the control Lib, the normal liver, and SMMC-7721 freezing tissue slices were used as controls.

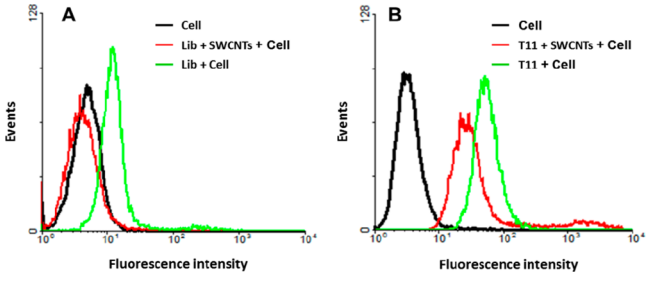

Figure 5. Binding of CNE2 with Lib (A) or aptamer T11 (B) before (green) and after (red) washing with SWCNTs. The concentration of probe is 500 nM.

Information).[39,40] Thus, based on these reasons, the SWCNTs would be more suitable to be employed in the cell-SELEX.

CONCLUSIONS

In summary, we have successfully developed a SWCNTs-assisted cell-SELEX method for generating aptamers based on the adsorption capacity of the SWCNTs. This method possesses some remarkable features, compared to the conventional cell-SELEX method. Highly affinitive and specific aptamers for target cells were achieved after only six selection rounds, which demonstrated improving selection efficiency. Moreover, a group of effective aptamers for CNE2 cells were generated successfully with the equilibrium dissociation constant (K_d) in the nanomolar range in our work. In addition, flow cytometry assay and confocal imaging results further verify that the selected aptamers can recognize the target CNE2 cells with high specificity. More importantly, truncated aptamers have been performed the ability of staining frozen tissue section, which demonstrated their potential application in clinical diagnosis and classification. Therefore, our strategy would provide a powerful research tool for the mechanism of the emergence, differentiation of cancer, and cancer metastasis.

ASSOCIATED CONTENT

Supporting Information

Additional information as noted in the text. This material is available free of charge via the Internet at http://pubs.acs.org.

AUTHOR INFORMATION

Corresponding Author

*Tel.: 86-731-88821566. Fax: 86-731-88821566. E-mail: kmwang@hnu.edu.cn.

Author Contributions

†These authors contributed equally to this work.

Notes

The authors declare no competing financial interest.

ACKNOWLEDGMENTS

This work was supported by the National Natural Science Foundation of China (Nos. 21175035, 21190040), National Basic Research Program (No. 2011CB911002), International Science & Technology Cooperation Program of China (No. 2010DFB30300), and Hunan Province Science and Technology Project of China (No. 2013FJ4042).

REFERENCES

(1) Tan, W. H.; Donovan, M. J.; Jiang, J. H. *Chem. Rev.* **2013**, *113*, 2842−2862.
(2) Liu, K. C.; Lin, B. S.; Lan, X. P. *J. Cell. Biochem.* **2013**, *114*, 250−255.
(3) Ellington, A. D.; Szostak, J. W. *Nature* **1990**, *346*, 818−822.
(4) Tuerk, C.; Gold, L. *Science* **1990**, *249*, 505−510.
(5) Shangguan, D. H.; Li, Y.; Tang, Z. W.; Cao, Z. C.; Chen, H. W.; Mallikaratchy, P.; Sefah, K.; Yang, C. J.; Tan, W. H. *Proc. Natl. Acad. Sci. U.S.A.* **2006**, *103*, 11838−11843.
(6) Tang, Z. W.; Shangguan, D. H.; Wang, K. M.; Shi, H.; Sefah, K.; Mallikratchy, P.; Chen, H. W.; Li, Y.; Tan, W. H. *Anal. Chem.* **2007**, *79*, 4900−4907.
(7) Zhao, Z. L.; Xu, L.; Shi, X. L.; Tan, W. H.; Fang, X. H.; Shangguan, D. H. *Analyst* **2009**, *134*, 1808−1814.
(8) Daniels, D. A.; Chen, H.; Hicke, B. J.; Swiderek, K. M.; Gold, L. *Proc. Natl. Acad. Sci. U.S.A.* **2003**, *100*, 15416−15421.
(9) Shangguan, D. H.; Meng, L.; Cao, Z. C.; Xiao, Z. Y.; Fang, X. H.; Li, Y.; Cardona, D.; Witek, R. P.; Liu, C.; Tan, W. H. *Anal. Chem.* **2008**, *80*, 721−728.

(10) Sefah, K.; Tang, Z. W.; Shangguan, D. H.; Chen, H.; Lopez-Colon, D.; Li, Y.; Parekh, P.; Martin, J.; Meng, L.; Phillips, J. A.; Kim, Y. M.; Tan, W. H. *Leukemia* **2009**, *23*, 235−244.
(11) Medley, C. D.; Bamrungsap, S.; Tan, W. H.; Smith, J. E. *Anal. Chem.* **2011**, *83*, 727−734.
(12) Bi, S.; Ji, B.; Zhang, Z. P.; Zhang, S. S. *Chem. Commun.* **2013**, *49*, 3452−3454.
(13) Liu, H. Y.; Xu, S. M.; He, Z. M.; Deng, A. P.; Zhu, J. J. *Anal. Chem.* **2013**, *85*, 3385−3392.
(14) Fang, X. H.; Tan, W. H. *Acc. Chem. Res.* **2010**, *43*, 48−57.
(15) Zhu, G. Z.; Ye, M.; Donovan, M. J.; Song, E. Q.; Zhao, Z. L.; Tan, W. H. *Chem. Commun.* **2012**, *48*, 10472−10480.
(16) Ye, M.; Hu, J.; Peng, M. Y.; Liu, J.; Liu, J.; Liu, H. X.; Zhao, X. L.; Tan, W. H. *Int. J. Mol. Sci.* **2012**, *13*, 3341−3353.
(17) Mallikaratchy, P.; Tang, Z. W.; Kwame, S.; Meng, L.; Shangguan, D. H.; Tan, W. H. *Mol. Cell. Proteomics* **2007**, *6*, 2230−2238.
(18) Cibiel, A.; Dupont, D. M.; Duconge, F. *Pharmaceuticals* **2011**, *4*, 1216−1235.
(19) Chang, Y. M.; Donovan, M. J.; Tan, W. H. *J. Nucleic Acids* **2013**, *2013*, 817350.
(20) Raddatz, M. S.; Dolf, A.; Endl, E.; Knolle, P.; Famulok, M.; Mayer, G. *Angew. Chem., Int. Ed.* **2008**, *47*, 5190−5193.
(21) Mayer, G.; Ahmed, M. S.; Dolf, A.; Endl, E.; Knolle, P. A.; Famulok, M. *Nat. Protoc.* **2010**, *5*, 1993−2004.
(22) Mendonsa, S. D.; Bowser, M. T. *J. Am. Chem. Soc.* **2004**, *126*, 20−21.
(23) Yang, J.; Bowser, M. T. *Anal. Chem.* **2012**, *85*, 1525−1530.
(24) Berezovski, M.; Musheev, M.; Drabovich, A.; Krylov, S. N. *J. Am. Chem. Soc.* **2006**, *128*, 1410−1411.
(25) Nie, H. Y.; Chen, Y.; Lu, C. C.; Liu, Z. *Anal. Chem.* **2013**, *85*, 8277−8283.
(26) Lou, X. H.; Qian, J. G.; Xiao, Y.; Viel, L.; Gerdon, A. E.; Lagally, E. T.; Atzberger, P.; Tarasow, T. M.; Heeger, A. J.; Soh, H. T. *Proc. Natl. Acad. Sci. U.S.A.* **2009**, *106*, 2989−2994.
(27) Qian, J. R.; Lou, X. H.; Zhang, Y. T.; Xiao, Y.; Soh, H. T. *Anal. Chem.* **2009**, *81*, 5490−5495.
(28) Huang, C. J.; Lin, H. I.; Shiesh, S. C.; Lee, G. B. *Biosens. Bioelectron.* **2012**, *35*, 50−55.
(29) Zheng, M.; Jagota, A.; Semke, E. D.; Diner, B. A.; McLean, R. S.; Lustig, S. R.; Richardson, R. E.; Tassi, N. G. *Nat. Mater.* **2003**, *2*, 338−342.
(30) Journet, C.; Maser, W. K.; Bernier, P.; Loiseau, A.; Lamy de la Chapelle, M.; Lefrant, S.; Deniard, P.; Lee, R.; Fischer, J. E. *Nature* **1997**, *388*, 756−758.
(31) Odom, T. W.; Huang, J. L.; Kim, P.; Lieber, C. M. *Nature* **1998**, *391*, 62−64.
(32) Jariwala, D.; Sangwan, V. K.; Lauhon, L. J.; Marks, T. J.; Hersam, M. C. *Chem. Soc. Rev.* **2013**, *42*, 2824−2860.
(33) Park, J. W.; Tatavarty, R.; Kim, D. W.; Jung, H. T.; Gu, M. B. *Chem. Commun.* **2012**, *48*, 2071−2073.
(34) Manna, S. K.; Sarkar, S.; Barr, J.; Wise, K.; Barrera, E. V.; Jejelowo, O.; Rice-Ficht, A. C.; Ramesh, G. T. *Nano Lett.* **2005**, *5*, 1676−1684.
(35) Tutak, W.; Park, K. H.; Vasilov, A.; Starovoytov, V.; Fanchini, G.; Cai, S. Q.; Partridge, N. C.; Sesti, F.; Chhowalla, M. *Nanotechnology* **2009**, *20*, 255101.
(36) Liu, Y.; Zhao, Y. L.; Sun, B. Y.; Chen, C. Y. *Acc. Chem. Res.* **2013**, *46*, 702−713.
(37) Yang, R. H.; Jin, J. Y.; Chen, Y.; Shao, N.; Kang, H. Z.; Xiao, Z. Y.; Tang, Z. W.; Wu, Y. R.; Zhu, Z.; Tan, W. H. *J. Am. Chem. Soc.* **2008**, *130*, 8351−8358.
(38) Britz, D. A.; Khlobystov, A. N. *Chem. Soc. Rev.* **2006**, *35*, 637−659.
(39) Wang, Y.; Li, Z. H.; Hu, D. H.; Lin, C. T.; Li, J. H.; Lin, Y. H. *J. Am. Chem. Soc.* **2010**, *132*, 9274−9276.
(40) Liang, H.; Zhang, X. B.; Lv, Y. F.; Gong, L.; Wang, R. W.; Zhu, X. Y.; Yang, R. H.; Tan, W. H. *Acc. Chem. Res.* **2014**, *47*, 1891−1901.
(41) Kunii, T.; Ogura, S.; Mie, M.; Kobatake, E. *Analyst* **2011**, *136*, 1310−1312.
(42) Song, Y. L.; Zhu, Z.; An, Y.; Zhang, W. T.; Zhang, H. M.; Liu, D.; Yu, C. D.; Duan, W.; Yang, C. J. *Anal. Chem.* **2013**, *85*, 4141−4149.